Radar Clutter Covariance Estimation: A Nonlinear Spectral Shrinkage Approach

SHASHWAT JAIN, Student Member, IEEE
VIKRAM KRISHNAMURTHY, Fellow, IEEE
Cornell University, Ithaca, NY USA

MURALIDHAR RANGASWAMY, Fellow, IEEE
Air Force Research Laboratory, Wright-Patterson AFB, OH USA

BOSUNG KANG, Member, IEEE
University of Dayton Research Institute, Dayton, OH USA

SANDEEP GOGINENI, Senior Member, IEEE
Information Systems Laboratories Inc., Dayton, OH USA

In this article, we exploit the spiked covariance structure of the clutter plus noise covariance matrix for radar signal processing. Using state-of-the-art techniques high dimensional statistics, we propose a nonlinear shrinkage-based rotation invariant spiked covariance matrix estimator. We state the convergence of the estimated spiked eigenvalues. We use a dataset generated from the high-fidelity, site-specific physics-based radar simulation software RFView to compare the proposed algorithm against the existing rank constrained maximum likelihood (RCML)-expected likelihood (EL) covariance estimation algorithm. We demonstrate that the computation time for the estimation by the proposed algorithm is less than the RCML-EL algorithm with identical Signal to Clutter plus Noise (SCNR) performance. We show that the proposed algorithm and the RCML-EL-based algorithm share the same optimization problem in high dimensions. We use Low-Rank Adaptive Normalized Matched Filter (LR-ANMF) detector to compute the detection probabilities for different false alarm probabilities over a range of target signal-to-noise ratios (SNR). We present preliminary results which demonstrate the robustness of the detector against contaminating clutter discretes using the challenge dataset from RFView. Finally, we empirically show that the minimum variance distortionless beamformer error variance for the proposed algorithm is identical to the error variance resulting from the true covariance matrix.

Manuscript received 6 February 2023; revised 24 April 2023; accepted 27 June 2023. Date of publication 4 July 2023; date of current version 8 December 2023.

DOI. No. 10.1109/TAES.2023.3292069

Refereeing of this contribution was handled by L. Rosenberg.

The work of S. Jain and V. Krishnamurthy was supported in part by the US Army Research Office under Grant W911NF-21-1-0093, in part by the Air Force Office of Scientific Research under Grant FA9550-22-1-0016, and in part by the National Science Foundation under Grant CCF-2312198. The work of M. Rangaswamy and B. Kang was supported by the Air Force Office of Scientific Research (AFOSR) under project 23RYCOR002. The work of S. Gogineni was supported by AFOSR under project 23RYCOR003.

Authors' addresses: Shashwat Jain and Vikram Krishnamurthy are with the Cornell University, Ithaca, NY 14853-0001, USA, E-mail: (sj474@cornell.edu; vikramk@cornell.edu); Muralidhar Rangaswamy is with the Air Force Research Laboratory, Wright-Patterson AFB, OH 45433-7132 USA, E-mail: (muralidhar.rangaswamy@us.af.mil); Bosung Kang is with the University of Dayton Research Institute, Dayton, OH 45469 USA, E-mail: (Bosung.Kang@udri.udayton.edu); and Sandeep Gogineni is with the Information Systems Laboratories Inc., Dayton, OH 45458 USA, E-mail: (sgogineni@islinc.com). *(Corresponding author: Vikram Krishnamurthy.)*

I. INTRODUCTION

Clutter plus noise covariance matrix estimation is an integral part of radar signal analysis. In a high-dimensional setting, the sample size is of the same order of magnitude as the dimension of the covariance matrix. Therefore, the sample covariance matrix is no longer a reliable estimator of the clutter plus noise covariance matrix as it becomes singular.

To mitigate such singular nature of the sample covariance matrix, we exploit the *spiked covariance structure* for high-dimensional settings proposed in [1], [2], and [3] to model the clutter plus noise covariance matrix. The *bulk* of the eigenvalues of the spiked covariance matrix are identical, corresponding to the noise component of the clutter plus noise covariance matrix. A finite number of *spiked* eigenvalues significantly exceed the *bulk* eigenvalues in magnitude, accounting for the clutter component of the clutter plus noise covariance matrix. We propose a rotation invariant nonlinear shrinkage-based spiked covariance estimator to estimate the clutter plus noise covariance matrix.

We use the challenge dataset contaminated with targets to validate our results. The challenge dataset was constructed by ISL[1] using high-fidelity, physics-based, site-specific, modeling, and simulation software RFView [4]. RFView uses stochastic transfer function model to simulate a scenario. It computes the Green's functions impulse response of the clutter and targets and simulates a real time instantiation of the RF environment. The RFView model accounts for intrinsic clutter motion encountered in the real world which existing models cannot address. This has been extensively vetted using measured data from VHF to X band with one case documented in [5] demonstrating the match with measured data. This provides the rationale for using the challenge dataset. The *spiked covariance* matrix structure can be observed in a real-world radar scenario. As an illustrative example, consider an airborne radar looking down on a heterogeneous terrain, consisting of mountains, water bodies, and foliage simulated by RFView, as shown in Fig. 1. Fig. 1 displays the relative power of the returned signal from such heterogeneous terrain in Southern California near San Diego. We observe that the regions of high-power returns

[1]Information Systems Laboratory (ISL) is a US based company that gave us access to the challenge dataset.

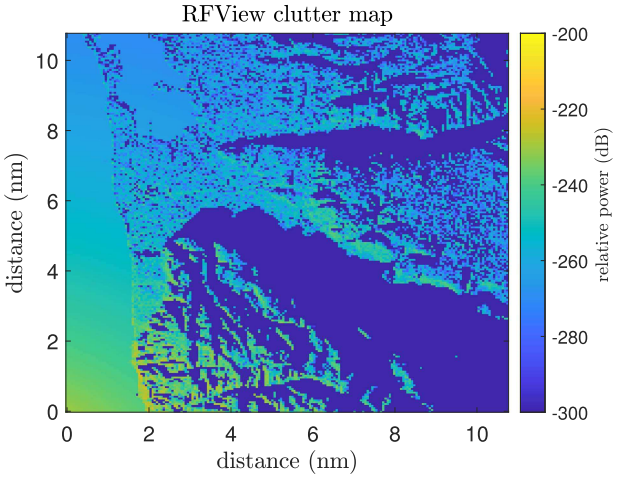

Fig. 1. Clutter returns from the littoral scene with mountains and water showing shadow regions (dark blue) as well as stronger signal components (yellow).

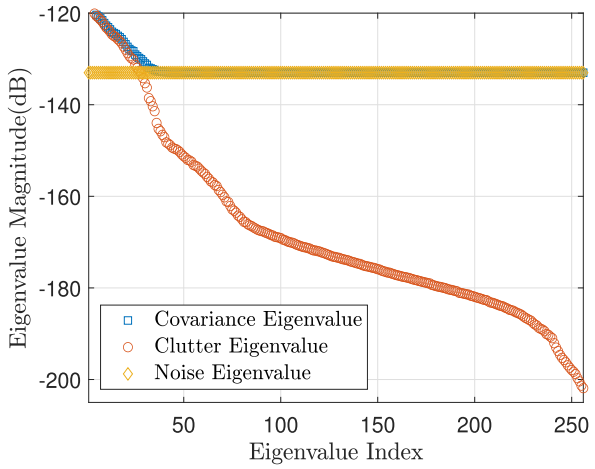

Fig. 2. Clutter plus noise covariance matrix formed by the return signal given in Fig. 1 gives evidence that most of the components of clutter (red) are below the noise floor. The first 25 components are above the noise floor. Therefore, the covariance matrix exhibits a spiked covariance structure.

have less area compared to the regions of low-power return, with noise power higher than the low-power returns. This is evident from the eigenvalue plot of the clutter plus noise covariance matrix in Fig. 2, computed from the return signal. A large number of eigenvalues of the clutter covariance matrix fall below the noise power.

In this article, we use a nonlinear shrinkage-based rotation invariant estimator developed in [3] to estimate the clutter plus noise covariance matrix in a high-dimensional setting. In the spiked covariance model, we only need to estimate the noise power and the spiked components.

We show that for the estimation of covariance matrix of dimension p, the proposed algorithm performs $\mathcal{O}(p)$ real-valued multiplications for the joint noise power-clutter rank estimation as compared to the $\mathcal{O}(p^2)$ in the RCML-EL[2] algorithm with identical SCNR and error variance. The proposed algorithm is applicable to adaptive radar where the covariance matrix computation speed up, as given in Table I, is beneficial during angle-Doppler sweeps over a region to detect targets. The angle-Doppler sweep requires repetitive batchwise computations of clutter plus noise covariance. The proposed algorithm reduces the clutter plus noise covariance computation time. Adaptive radars also have several hierarchical layers for data acquisition, processing, and decision-making [8]. The reduced clutter plus noise covariance computation time is beneficial since it relaxes time constraints for other hierarchical layers which include target tracking, beam allocation, pulse shaping [9], task scheduling, and resource allocation, as stated in [10].

In addition, we state the convergence results for the estimated eigenvalues and bounds for normalized SCNR for the proposed estimator. We test the target detection performance of the estimator using low-rank adaptive normalized matched filter (LR-ANMF) detector. We empirically show the robustness of the detector against contaminating clutter discretes. We apply the proposed algorithm on the challenge dataset simulated by RFView software.

A. Related Works

The problem of covariance matrix estimation [11], with data deficient scenario has received considerable attention in radar signal processing literature. In the data deficient scenarios, the sample covariance matrix is no longer a reliable estimator as it becomes ill-conditioned. To address such ill-conditioning, methods like diagonal loading (DL) [12], [13], [14], [15], [16], [17], [18] and factored space-time approaches [19] have been proposed. Data dependent techniques include principal components inverse [20], multistage Wiener filter [21], parametric adaptive matched filter [22], and EigenCanceler [23]. Data independent approaches include JDL-GLR [24].

In a high-dimensional setting, the properties of covariance matrices are explained by the random matrix theory, as stated in [25], [26], [27], and [28]. In such high-dimensional settings, shrinkage estimators have been developed to estimate covariance matrices in signal processing and finance. Shrinkage estimators have been used in wireless communications [29] to estimate the channel matrices, in array signal processing to estimate direction of arrival [30] and in finance for Markowitz portfolio optimization [31], [32], [33], [34]. Shrinkage methods include Ledoit–Wolf shrinkage estimator [35], regularized PCA [36], Ridge and Lasso shrinkage estimators [37], and regularized M-estimators [38].

In radar signal processing, the covariance matrices often contain a low-rank structure corresponding to the clutter.

[2]RCML-ELrepresents the RCML covariance estimator [6] with the clutter rank and noise power obtained by the expected likelihood (EL) approach [7].

The covariance matrices are called clutter plus noise covariance matrices. Covariance estimation algorithms developed in [7], [39], [40], [41], and [42], propose estimation schemes assuming a rank sparse clutter covariance matrix in a high-dimensional setting. These papers use the Brennan's rule which gives an estimate of the rank depending on the dominant components of the clutter and the jammers. However, as demonstrated in [43], [44], and [45], the Brennan's rule fails when a plethora of real-world effects, such as internal clutter motion, mutual coupling between antenna array elements arise on account of the system and environmental factors. In our article, the data generated from the high fidelity, site-specific, physics-based, radar scenario simulation software RFview are used where the Brennan rule does not prevail, as documented in [5].

To address these issues we exploit the *spiked covariance* structure, as proposed in [1], [2], [46], and [47], of the clutter plus noise covariance matrix. We use the nonlinear shrinkage estimation techniques of [3] to estimate the covariance matrix. Spiked covariance models have been used to estimate direction of arrival (DOA) in array signal processing, as demonstrated in [48], and for target detection in [49]. We are using the spiked covariance model to estimate the clutter plus noise covariance matrix.

B. Main Results and Organization

The main results and organization of this article are as follows.

1) In Section II-A, we formulate the rotation invariant estimators. The asymptotic model for large random matrices and the spiked covariance model for the clutter plus noise covariance matrix is defined in Section II-B.
2) In Section III, we present the algorithm proposed in [3] for spiked covariance matrix estimation. In Section III-A, Theorem 1 shows a strong law of large numbers (namely, the estimated spiked eigenvalues converge almost surely to a constant) and satisfy a central limit theorem. This is due to the fact that, even though we are in a high-dimensional setting, the number of spikes is constant. Empirical verification of the convergence properties for RFview Challenge Dataset is provided. We derive the bounds for normalized SCNR ρ in Section III-B. In Section III-C, we establish that the proposed algorithm and the RCML-EL estimation algorithm in high dimensions have similar performance due to the fact they share a common optimization problem. In Section III-D, we employ the LR-ANMF detector to verify target detection performance when using a rotation invariant estimator.
3) In Section IV-A, we demonstrate that the proposed algorithm has identical SCNR compared to the RCML-EL algorithm for the challenge dataset simulated using RFView. We further show that the computation time of estimation by the proposed algorithm is less than that of the RCML-EL algorithm. In Section IV-B, we compute the target detection probabilities for various false alarm probabilities and SCNR, and empirically show its robustness with respect to contaminating clutter discretes. In Section IV-C, we compute the error variance of the minimum variance distortionless beamformer (MVDR) beamformer for the proposed algorithm.

II. ROTATION INVARIANT ESTIMATOR AND SPIKED COVARIANCE MODEL

This section is organized as follows. Section II-A presents a general rotation invariant estimator. Section II-B describes the high-dimensional spiked covariance model.

We use a narrowband baseband equivalent model used in [5]. The radar transmits a complex-valued waveform $s(k)$ and receives a complex-valued return $y(k)$ in discrete time

$$y(k) = h_t(k) \circledast s(k) + h_c(k) \circledast s(k) + n(k). \tag{1}$$

Here $\circledast$ is the convolution operator and k denotes discrete time. $h_t(k)$ and $h_c(k)$ are the complex valued target impulse response and complex valued clutter impulse response, respectively. The noisy measurement $n(k)$, due to thermal noise, is the additive white Gaussian noise with variance σ^2 with zero mean. The noise samples are independent, identically, distributed $(i.i.d)$.

In matrix-vector notation, (1) reads

$$\mathbf{y} = \mathbf{H}_t\,\mathbf{s} + \mathbf{H}_c\,\mathbf{s} + \mathbf{n}_s \tag{2}$$

where $\mathbf{H}_t,\ \mathbf{H}_c \in \mathbb{C}^{p\times q}$ are Toeplitz matrices constructed by the impulse responses $h_t(k)$ and $h_c(k)$, respectively. $\mathbf{y} \in \mathbb{C}^p$ is a return signal of length p and $\mathbf{s} \in \mathbb{C}^q$ is the waveform of pulse length q. The noise $\mathbf{n}_s \in \mathbb{C}^p$ is a complex valued Gaussian distributed vector, where $\mathbf{n}_s \sim \mathcal{N}(\mathbf{0}, \sigma^2\,\mathbf{I})$ and has $i.i.d$ samples.

We define the clutter plus noise return as $\mathbf{y}_c$

$$\mathbf{y}_c := \mathbf{H}_c\,\mathbf{s} + \mathbf{n}_s. \tag{3}$$

A. Rotation Invariant Estimator

In this subsection, we describe the rotation invariant estimation for the clutter plus noise covariance matrix. Rotation invariant estimators have the same eigenvectors as that of the sample covariance matrix and the eigenvalues of the estimators are a function of the eigenvalues of the sample covariance matrix.

The clutter plus noise covariance matrix is given by

$$\mathbf{R} = \mathbf{R}_c + \sigma^2\,\mathbf{I} \tag{4}$$

where the clutter covariance matrix is

$$\mathbf{R}_c := \mathbb{E}[\mathbf{H}_c\,\mathbf{s}\mathbf{s}^H\,\mathbf{H}_c{}^H] \tag{5}$$

and $\sigma^2\,\mathbf{I}$ is the noise component. The eigendecomposition of clutter plus noise covariance is

$$\mathbf{R} = \sum_{i=1}^{p} \lambda_i \mathbf{u}_i \mathbf{u}_i^H \tag{6}$$

with eigenvalues λ_i and eigenvectors $\mathbf{u}_i$. The sample covariance matrix $\hat{\mathbf{R}}_n$ is

$$\hat{\mathbf{R}}_n = \frac{1}{n}\sum_{k=1}^{n} \mathbf{y}_{c,k}\,\mathbf{y}_{c,k}^H \tag{7}$$

where $\mathbf{y}_c$ is the clutter plus noise return defined in (3) which will be used as training data samples, k is the discrete time, and n are the number of training data samples. The spectral decomposition of $\hat{\mathbf{R}}_n$ for a given training data size n is

$$\hat{\mathbf{R}}_n = \sum_{i=1}^{p} \hat{\lambda}_{i,n}\mathbf{v}_{i,n}\,\mathbf{v}_{i,n}^H \tag{8}$$

where $\hat{\lambda}_{i,n}$ are the eigenvalues and $\mathbf{v}_{i,n}$ are the eigenvectors of $\hat{\mathbf{R}}_n$. The spiked covariance matrix estimate for a given number of data samples n is

$$\bar{\mathbf{R}}_n = \sum_{i=1}^{p} \bar{\lambda}_{i,n}\,\mathbf{v}_{i,n}\,\mathbf{v}_{i,n}^H \tag{9}$$

where $\bar{\lambda}_{i,n}$ are the eigenvalues of $\bar{\mathbf{R}}_n$, with eigenvectors $\mathbf{v}_{i,n}$ identical to those of the $\hat{\mathbf{R}}_n$ in (8). The spiked covariance estimator is a rotation invariant estimator.

In addition, we use normalized SCNR to compare covariance estimation methods. We denote ρ to define the normalized SCNR as

$$\rho = \frac{(\mathbf{y}_t{}^H\,\bar{\mathbf{R}}^{-1}\,\mathbf{y}_t)^2}{(\mathbf{y}_t{}^H\,\mathbf{R}^{-1}\,\mathbf{y}_t)(\mathbf{y}_t{}^H\,\bar{\mathbf{R}}^{-1}\,\mathbf{R}\,\bar{\mathbf{R}}^{-1}\,\mathbf{y}_t)}. \tag{10}$$

where $\mathbf{y}_t = A_\theta \otimes A_f$ is the Kronecker product of angle steering vector $[A_\theta]_i = \exp[-j\pi i \sin(\theta)]$, $1 \le i \le N$ and the Doppler steering vector $[A_f]_i = \exp[-j2\pi i f_d]$, $1 \le i \le K$. N and K are defined in Section IV. The dimension of the covariance matrix is $p = N \times K$.

In the next section, we will show that $\bar{\lambda}$ is a nonlinear function of $\hat{\lambda}$, where the nonlinearity depends on the loss function.

B. Clutter Plus Noise Covariance Matrix Modeling Using Large Random Matrices

In this subsection, we define the spiked covariance model and the asymptotic regime for the high-dimensional setting. We use this framework to model the clutter plus noise covariance matrix.

DEFINITION 1 A spiked covariance matrix $\mathbf{R}$ is a $p \times p$ positive definite Hermitian matrix with eigenvalues $(\lambda_1, \lambda_2 \ldots, \lambda_p)$ such that for a finite $r \ll p$, $\lambda_1 \ge \lambda_2 \ge \lambda_r > \sigma^2$ and $\lambda_{r+1} = \cdots = \lambda_p = \sigma^2 > 0$.

We make two assumptions

1) The clutter plus noise covariance matrix has a spiked covariance structure given in Definition 1. The clutter plus noise covariance matrix is given in (4), where clutter covariance matrix $\mathbf{R}_c$ has rank r with eigenvalues $\lambda_i - \sigma^2$, $1 \le i \le r$. The noise covariance matrix $\sigma^2\,\mathbf{I}$ is diagonal.
2) There exists a $\gamma \in (0, 1)$ such that for given training data size n with the dimension of the covariance matrix as p such that

$$\frac{p}{n} \to \gamma, \quad p, n \to \infty, \quad p < n. \tag{11}$$

Data displayed in Figs. 1 and 2 satisfies these conditions. In Fig. 2, we see that the clutter covariance matrix can be approximated by a rank r positive semidefinite matrix as the remaining $p - r$ components are below the noise floor.

We assume that clutter plus noise covariance matrix is spiked if the rank of the clutter matrix is less than a fraction χ of the clutter plus noise covariance matrix. For convenience, we choose $\chi = 0.1$, since it empirically fits with the data simulated by RFView. In the classical statistical setting, this is well studied in terms of penalized likelihood methods, such as Akaike information criterion (AIC) [50], minimum description length (MDL) [51], information theoretic criteria [52], statistical techniques [53], data dependent techniques [54], and min-max approaches, such as the embedded exponential families [55].

However, in the high-dimensional setting considered in this article, estimating the model order (number of spikes) is a difficult problem and will not be addressed. In [7], the RCML-EL algorithm uses the Brennan's rule [11], as an initial estimate for the rank of the clutter covariance matrix to determine the model order. RCML-EL algorithm correctly estimates the rank as compared to the AIC and MDL techniques. In Section III-C, since the proposed algorithm and RCML-EL algorithm share similar optimization problem, the proposed algorithm correctly estimates the model order.

The spiked covariance property helps us to deal with the clutter plus noise covariance matrices in high dimensions, which is frequently encountered in radar signal processing. With this knowledge, we define the nonlinear shrinkage-based rotation invariant estimator.

III. NONLINEAR SHRINKAGE ESTIMATION

In this section, we propose the rotation invariant estimator using nonlinear shrinkage of the eigenvalues of the sample covariance matrix. We state the convergence of the estimated eigenvalues in Theorem 1 in Section III-A. Note that we use the terms spiked eigenvalues and the leading r eigenvalues of the covariance matrix interchangeably for a fixed clutter covariance matrix with rank r. We outline the computation cost of the proposed algorithm. We propose bounds for the normalized SCNR(ρ) in Section III-B. We show the similarity of SCNR performance between the proposed algorithm and the RCML-EL algorithm in high dimensions in Section III-C. We conclude this section by stating the ANMF for target detection for the proposed algorithm in Section III-D.

The spiked covariance matrix $\mathbf{R}$ is stated in Definition 1. Estimation of the spiked covariance matrix $\bar{\mathbf{R}}_n$, as defined in (9), consists of two subproblems: estimation of the spiked eigenvalues and the estimation of the noise power σ^2.

1) The estimate of the noise power is given, as stated in [3], is

$$\hat{\sigma}^2 = \frac{\hat{\lambda}_{\text{med}}}{\mu_{\text{med}}} \tag{12}$$

where $\hat{\lambda}_{\text{med}}$ is the median of the eigenvalues of the sample covariance matrix $\hat{\mathbf{R}}_n$ and μ_{med} is the median of the Marchenko–Pastur distribution with parameter γ stated in (11). The proof of the consistency of the noise power estimator is given in [3, Sec. 9].

2) The shrinkage function $\eta^*(\cdot)$, as stated in [3], is

$$\eta^*(\tilde{\lambda}_i) = \begin{cases} \eta(f(\tilde{\lambda}_i)) & \tilde{\lambda}_i > (1+\sqrt{\gamma})^2 \\ 1 & \tilde{\lambda}_i \le (1+\sqrt{\gamma})^2 \end{cases} \tag{13}$$

where $\tilde{\lambda}_i = \hat{\lambda}_i/\hat{\sigma}^2$, $\hat{\lambda}_i$ are the eigenvalues of the sample covariance matrix $\hat{\mathbf{R}}$ and $\hat{\sigma}^2$ is defined in (12). The function $f(\cdot)$ given by[3]

$$f(x) = \frac{x+1-\gamma+\sqrt{(x+1-\gamma)^2-4x}}{2} \tag{15}$$

and $\eta(\cdot)$ for Stein loss, as stated in [3], $\mathrm{L}^{St} = \mathrm{tr}(\mathbf{R}^{-1}\bar{\mathbf{R}} - \mathbf{I}) - \log\det(\mathbf{R}^{-1}\bar{\mathbf{R}})$, is given by

$$\eta^{\text{St}}(x) = \frac{x}{c(x)^2 + s(x)^2 x} \tag{16}$$

where $c(\cdot)$ is given by

$$c(x) = \begin{cases} \sqrt{\frac{1-\gamma/(x-1)^2}{1+\gamma/(x-1)}} & x > 1+\sqrt{\gamma} \\ 0 & x \le 1+\sqrt{\gamma} \end{cases} \tag{17}$$

$s(\cdot)^2 = 1 - c(\cdot)^2$ and γ is given in (11).
The eigenvalues $\bar{\lambda}_{i,n}$ of the estimator $\bar{\mathbf{R}}_n$ are given by

$$\bar{\lambda}_{i,n} = \hat{\sigma}^2\,\eta^*(\tilde{\lambda}_i) \tag{18}$$

where $\hat{\sigma}^2$ is given in (12) and $\eta^*(\tilde{\lambda}_i)$ is given in (13). The proof of optimality of this estimator is given in [3, Sec. 6].

A pseudo-code to compute the estimator is stated in Algorithm 1.

Algorithm 1: Nonlinear Shrinkage Algorithm for Spiked Covariance Matrix Estimation.

1: Evaluate the eigenvalue decomposition of sample covariance matrix $\hat{\mathbf{R}}_n$ as done in (8) for a given number of data samples n.
2: Compute the noise power $\hat{\sigma}^2$ by (12).
3: Compute the eigenvalues $\bar{\lambda}_{i,n}$ of the estimator as in (18).
4: Using eigenvalues computed in Step 3, the estimated covariance matrix $\bar{\mathbf{R}}_n$ is given by (9).

A. Convergence of Eigenvalues of the Proposed Estimator

Although we deal with finite p and n, in Theorem 1 we state that the spiked eigenvalues converge almost surely to a constant and satisfy a central limit theorem when both $p, n \to \infty$, given that the number of spikes r is fixed.

We assume the following for a covariance matrix $\mathbf{R}$ with dimension p.

A1. Leading r distinct eigenvalues $\lambda_1, \lambda_2, \ldots, \lambda_r$ with multiplicity 1 and lower bounded by $1+\sqrt{\gamma}$.
A2. Eigenvalues $\lambda_{r+1} = 1, \ldots, \lambda_p = 1$.

THEOREM 1 Consider the estimator $\bar{\mathbf{R}}_n$ of dimension p with eigenvalues $(\bar{\lambda}_{1,n}, \bar{\lambda}_{2,n}, \ldots, \bar{\lambda}_{p,n})$ that estimates the spiked covariance matrix $\mathbf{R}$ satisfying the assumptions (A1) and (A2). Assume $p/n \to \gamma \in (0,1)$, $p, n \to \infty$. Then $\bar{\lambda}_{i,n}$'s, $1 \le i \le r$ satisfy

$$\bar{\lambda}_{i,n} \xrightarrow{a.s.} \eta^*(\beta_i). \tag{19}$$

In addition, if $p/n - \gamma = o(n^{-1/2})$, then

$$\sqrt{n}(\bar{\lambda}_{i,n} - \eta^*(\beta_i)) \xrightarrow{d} \mathcal{N}(0, \alpha_i^2\,(\eta'(\beta_i))^2) \tag{20}$$

where $\eta^*(\cdot)$ is given by (13) and $\eta(\cdot)$ is given by (16). $\beta_i = \lambda_i + \frac{\gamma\lambda_i}{\lambda_i - 1}$, $\alpha_i^2 = 2\lambda_i^2(1 - \frac{\gamma}{(\lambda_i-1)^2})$ and γ is given (11).

PROOF Almost sure convergence can be proved by applying continuous mapping theorem on [2, Th. 2] with function η. The in-distribution convergence can be proved by applying the delta method on [2, Th. 3] with function η. ■

We empirically showed the validity of assumptions of Theorem 1 for the challenge dataset using the double version of the Kolmogorov–Smirnov (K–S) test with significance level 5% and 1024 Monte Carlo simulations. The reference data was generated from the prescribed distribution in (20) and the test data were generated from the challenge dataset. The cumulative distribution function (CDF) plot in Fig. 3 for the test and reference data reveals that the challenge dataset satisfies the assumptions for Theorem 1.

Computation Cost

Algorithm 1 does not require prior knowledge of the number of spikes. Step (2) and Step (3) in Algorithm 1 determine the eigenvalues that are above the noise floor. The computation cost of the algorithm is given as follows.

1) The eigenvalue decomposition requires $\mathcal{O}(p^3)$ real-valued multiplications.
2) The noise power estimation, step (2), is a median finding algorithm that requires $O(p)$ real-valued multiplications.
3) The nonlinear shrinkage, step (3), requires $\mathcal{O}(r)$ real-valued multiplications, r being the rank of the clutter covariance matrix.

[3]It is to be noted that (15) is the inverse mapping for

$$g(x) = \begin{cases} x + \frac{\gamma x}{x-1} & x > 1+\sqrt{\gamma} \\ (1+\sqrt{\gamma})^2 & 1 \le x \le 1+\sqrt{\gamma} \end{cases} \tag{14}$$

when $x > (1+\sqrt{\gamma})^2$, it is the relationship between the $\hat{\lambda}$ and λ and has been explained in [3].

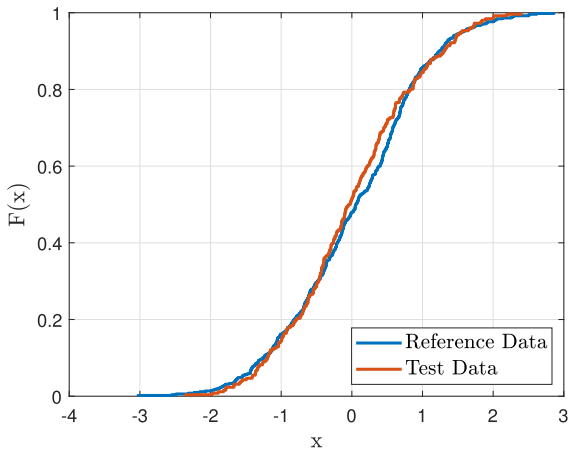

Fig. 3. Double version of the K–S test with reference data from the prescribed distribution (20) and the test data from the challenge dataset verifies that the challenge dataset satisfies the assumptions for Theorem1 with p-value of 0.8390.

We compare Algorithm 1 to the RCML-EL algorithm whose computational cost is given as follows.

1) The eigenvalue decomposition step takes $\mathcal{O}(p^3)$ real valued multiplications.
2) The joint noise and rank estimation step takes $\mathcal{O}(p^2)$ real valued multiplications.

The difference is in the noise and rank estimation step; Algorithm 1 takes $\mathcal{O}(p)$ real-valued multiplications, whereas the RCML-EL algorithm takes $\mathcal{O}(p^2)$. This will be demonstrated in Section IV-A empirically.

B. Bounds for ρ

In this section, we derive the lower and upper bounds for the normalized SCNR(ρ) using results from [56].

We rewrite ρ from (10)

$$\rho = \frac{\|\mathbf{x}\|_2^2}{(\mathbf{x}^H \bar{\mathbf{R}}^{-\frac{1}{2}} \mathbf{R} \bar{\mathbf{R}}^{-\frac{1}{2}} \mathbf{x})(\mathbf{x}^H \bar{\mathbf{R}}^{\frac{1}{2}} \mathbf{R}^{-1} \bar{\mathbf{R}}^{\frac{1}{2}} \mathbf{x})} \tag{21}$$

where $\mathbf{x} = \hat{\mathbf{R}}^{-\frac{1}{2}} \mathbf{y}_t$. Without loss of generality, assume $\|\mathbf{x}\| = 1$. We use the matrix version of Kantorovich's inequality to bound the denominator. For a positive semidefinite matrix $\mathbf{A}$ and a unit vector $\mathbf{x}$, $\|\mathbf{x}\|_2 = 1$, $(\mathbf{x}^H \mathbf{A} \mathbf{x})(\mathbf{x}^H \mathbf{A}^{-1} \mathbf{x}) \leq \frac{1}{4}(\kappa(\mathbf{A}) + \frac{1}{\kappa(\mathbf{A})} + 2)$, where $\kappa(\mathbf{A})$ is the condition number of the matrix A. By the Cauchy–Schwarz inequality $(\mathbf{x}^H \mathbf{A} \mathbf{x})(\mathbf{x}^H \mathbf{A}^{-1} \mathbf{x}) \geq 1$. We lower bound ρ by

$$\rho \geq \frac{1}{\frac{1}{4}(\kappa(\mathbf{A}) + \frac{1}{\kappa(\mathbf{A})} + 2)} \tag{22}$$

where $\mathbf{A} = \bar{\mathbf{R}}^{-\frac{1}{2}} \mathbf{R} \bar{\mathbf{R}}^{-\frac{1}{2}}$. From [56], we have

$$\kappa(\mathbf{A}) = \frac{\max\left[1, \max_{1 \leq i \leq r} \nu_+(\lambda_i^*, \eta_i)\right]}{\min\left[1, \min_{1 \leq i \leq r} \nu_-(\lambda_i^*, \eta_i)\right]} \tag{23}$$

where

$$\nu_\pm(\lambda_i^*, \eta_i) = T/2 \pm \sqrt{T^2/4 - D}$$

$$D = \eta^{\mathrm{St}}/\lambda^*, \quad T = \left(\frac{s^2 + \eta^{\mathrm{St}} c^2}{\lambda^*} + c^2 + \eta^{\mathrm{St}} s^2\right)$$

η^{St} defined in (16) and $\lambda_i^* = \lambda_i/\sigma^2$.

In Section IV, we shall demonstrate that the proposed algorithm performs within the derived bounds.

C. Performance Similarity Between Proposed Algorithm and RCML-EL Algorithm

In this section, we show that the proposed algorithm and the RCML-EL algorithm will give similar SCNR performance.

The optimization problem for clutter plus noise covariance matrix estimation assuming noise power to be unity defined in [6, (35)] is

$$\begin{aligned} \min_{\bar{\boldsymbol{\lambda}}} \quad & \mathbf{d}^T \bar{\boldsymbol{\lambda}} - \mathbf{1}^T \log \bar{\boldsymbol{\lambda}} \\ \text{s.t.} \quad & \mathbf{F} \bar{\boldsymbol{\lambda}} \preceq \mathbf{g} \\ & \mathbf{E} \bar{\boldsymbol{\lambda}} = \mathbf{h} \end{aligned} \tag{24}$$

where $d_i = \hat{\lambda}_i$, recall from Section II that $\bar{\lambda}$ is eigenvalue of the estimator and $\hat{\lambda}$ is the eigenvalue of the sample covariance matrix

$$\mathbf{F} = \begin{bmatrix} \mathbf{U}^{\mathbf{T}} & -\mathbf{I}_{p \times p} & \mathbf{I}_{p \times p} \end{bmatrix}^T \in \mathbb{R}^{3p \times p}$$

$$\mathbf{g} = \begin{bmatrix} \mathbf{0}_{p \times 1}^T & -\boldsymbol{\epsilon}_{p \times 1}^T & \mathbf{1}_{p \times 1}^T \end{bmatrix}^T \in \mathbb{R}^{3p \times 1}$$

$\boldsymbol{\epsilon}_{p \times 1} = [\epsilon, \ldots, \epsilon]_{p \times 1}$, $\epsilon > 0$,

$$\mathbf{U} = \begin{bmatrix} 1 & -1 & 0 & 0 & \ldots & 0 \\ 0 & 1 & -1 & 0 & \ldots & 0 \\ \vdots & \ddots & \ddots & \ddots & \vdots & \vdots \\ 0 & \ldots & \ldots & \ldots & 1 & -1 \end{bmatrix} \in \mathbb{R}^{p \times p}$$

$$\mathbf{E} = \begin{bmatrix} \mathbf{0}_{r \times r} & \mathbf{0}_{r \times p-r} \\ \mathbf{0}_{(p-r) \times r} & \mathbf{I}_{p-r} \end{bmatrix} \in \mathbb{R}^{p \times p}$$

$$\mathbf{h} = \begin{bmatrix} 0, & 0, & \ldots, 0_r, & 1, & 1, \ldots, 1 \end{bmatrix}^T \in \mathbb{R}^{p \times 1}.$$

The first constraint in (24) enforces $\bar{\lambda}_i$ to be positive in descending order and the second constraint enforces the last $p - r$ eigenvalues of the estimator to be equal. These constraints enforce a spiked covariance matrix structure on the estimator, stated in Definition 1, in a high-dimensional setting. In [3], the optimization problem for estimating leading r eigenvalues for Stein loss under a spiked covariance model is given by

$$\min_{\bar{\lambda}_i,\, 1 \leq i \leq r} \quad a_i \bar{\lambda}_i - b_i \log \bar{\lambda}_i + m_i \tag{25}$$

where $a_i = c^2/g(\hat{\lambda}_i) + s^2$, $b_i = 1$ and $m_i = 1/g(\hat{\lambda}_i) - 1 - a_i + \log(f(\hat{\lambda}_i))$; $f(\cdot)$ is given in (15), $g(\cdot)$ is given in (14), $c(\cdot)$ and $s(\cdot)$ are given in (17).

Since the cost function of (24) is identical to (25) within a constant and the constraints of (24) are implicit to the

optimization problem of (25), the normalized SCNR, ρ and the rank of the clutter covariance matrix r will be identical.

In Section IV, we shall demonstrate that the SCNR performance for the proposed algorithm is identical to the RCML-EL algorithm with a reduced computation time.

D. Low-Rank Adaptive Normalized Matched Filter Detection

In this section, we use the LR-ANMF detector for a rotation-invariant estimator, as stated in [57]. The detection scheme is independent of the eigenvalue shrinkage in (13) and only depends on the eigenvectors of the sample covariance matrix in high dimensions. The detector is the same for both the proposed algorithm and the RCML-EL algorithm.

We have the following binary hypothesis for a single target:

$$\begin{aligned}\mathcal{H}_0 &: \mathbf{y} \sim \mathcal{N}(0, \mathbf{R}) \\ \mathcal{H}_1 &: \mathbf{y} \sim \mathcal{N}(h_t \mathbf{s}, \mathbf{R})\end{aligned} \tag{26}$$

where $\mathcal{H}_0$ is the null hypothesis when no target is present and $\mathcal{H}_1$ is the alternate hypothesis when the target is present. The target signal $\mathbf{s}$ is defined in the same way as $\mathbf{y}_t$ in (10) with a complex-valued amplitude h_t and $\mathbf{R}$ is the clutter plus noise covariance matrix. The test statistics for the LR-ANMF with n data samples, as stated in [58], is

$$T_n = \frac{|\mathbf{s}\,\hat{\Pi}_n\,\mathbf{y}|^2}{\|\hat{\Pi}_n\,\mathbf{s}\|^2} > \delta \tag{27}$$

where

$$\hat{\Pi}_n = \mathbf{I} - \sum_{i=1}^{r} \mathbf{v}_{i,n}\,\mathbf{v}_{i,n}^H$$

is a projection matrix constructed using the eigenvectors $\mathbf{v}_{i,n}$ defined in (8) corresponding to the r spikes of the spiked covariance matrix and δ is the detection threshold. Recall from Section II-B that r is the rank of the clutter covariance matrix. The knowledge of noise power σ^2 is not impacting the detection since we are using assumption (A1) in Section III-A, where σ^2 has already been estimated. We present the convergence theorems from [57] that state the in-distribution convergence of the test statistics under $\mathcal{H}_0$ and $\mathcal{H}_1$.

THEOREM 2 ([57], TH. 2) Under $\mathcal{H}_0$ and assumption (A1) the test statistics T_n satisfies

$$T_n \xrightarrow{D} \chi^2(2) \tag{28}$$

where $\chi^2(2)$ is a chi-squared distribution with one complex degree of freedom. The probability of false alarm with detection threshold δ is

$$\begin{aligned}{}_{FA} &= \lim_{n\to\infty} \mathbb{P}(T_n > \delta|\mathcal{H}_0) = \int_{\delta}^{\infty} \exp(-x)\,dx \\ &= \exp(-\delta).\end{aligned} \tag{29}$$

THEOREM 3 ([57], TH. 3): Under $\mathcal{H}_1$ and assumption (A1) the test statistics T_n satisfies

$$\lim_{n\to\infty} \sup_{x\in\mathbb{R}} |\mathbb{P}(T_n < x) - F(x; 2, \Delta)| \to 0 \tag{30}$$

where $F(x; 2, \Delta)$ denotes the cumulative distribution of a noncentral χ^2 distribution with one complex degree of freedom and noncentrality parameter Δ

$$\Delta = \frac{2|h_t|^2}{\nu}. \tag{31}$$

h_t is defined in (26)

$$\begin{aligned}\nu = &\frac{1}{\|\Pi\mathbf{s}\|^2 + \sum_{i=1}^{r}(1 - c^2(\lambda_i))|\mathbf{s}^H\,\mathbf{u}_i|^2} \\ &+ \frac{\sum_{i=1}^{r}(\lambda_i - 1)(1 - c^2(\lambda_i))|\mathbf{s}^H\,\mathbf{u}_i|^2}{(\|\Pi\mathbf{s}\|^2 + \sum_{i=1}^{r}(1 - c^2(\lambda_i))|\mathbf{s}^H\,\mathbf{u}_i|^2)^2}\end{aligned}$$

where $\Pi = \mathbf{I} - \sum_i^r \mathbf{u}_i\mathbf{u}_i^H$, $c(\cdot)$ is defined in (17), $\mathbf{u}_i$ defined in (6), r is rank of the clutter covariance matrix, and $\mathbf{s}$ defined in (26). The corresponding target detection probability with detection threshold δ is

$$\begin{aligned}P_D &= \exp(-\Delta)\sum_{k=0}^{\infty}\frac{\Delta^k}{k!}\left[1 - \frac{\int_0^{\delta} x^k \exp(-x)\,dx}{\Gamma(k+1)}\right] \\ &= \lim_{n\to\infty} \mathbb{P}(T_n > \delta|\mathcal{H}_1)\end{aligned} \tag{32}$$

where $\Gamma(\cdot)$ is the gamma function.

In Section IV-B, we compute the detection probabilities for different false alarm probabilities over a range of signal-to-noise ratios (SNRs), we empirically evaluate the robustness of the detector for detecting a single target in the presence of multiple targets that act as contaminating clutter discretes. Contaminating clutter discretes are additional spikes that are present due to undesired targets. They are not part of clutter spikes and change the clutter covariance matrix rank from r to $\hat{r}$.

To conclude this section, we propose the nonlinear shrinkage-based rotation invariant estimator by using the sample covariance matrix. We state the convergence of the spiked eigenvalues of the estimator. We state the bounds for the normalized SCNR. The equivalence of the RCML-EL algorithm in a high-dimensional setting to the proposed algorithm is established. A detector for target detection is stated for the proposed algorithm.

IV. NUMERICAL EXAMPLES

We use a dataset generated using RFView software that provides an accurate characterization of complex RF environments. It uses stochastic transfer functions [5] to simulate the high-fidelity RF clutter encountered in practice.

The dataset consists of a data cube in the time domain and is a multidimensional $N \times K \times n$ matrix, where N is the total number of channels, K is the slow time, and n is the number of range gates (fast-time) in a specified coherent processing interval. For our case, we use the range gates as the number of data samples n.

TABLE I
Algorithm 1 Takes Less Computation Time as Compared to the RCML-EL Algorithm for the Challenge Data Set

Training Data Size (n)	Proposed	RCML-EL	Speed Up
512	0.012035 s	0.107116 s	9×
1024	0.003046 s	0.070876 s	23×
1536	0.002028 s	0.053037 s	26×
2048	0.002026 s	0.050819 s	25×
2560	0.002090 s	0.050504 s	24×

It is to be noted that the speed-up factor depends on the processor parameters, which varies from machine to machine.

In Section IV-A, we use the challenge dataset generated by RFView. We compare the performance of the Algorithm 1 against the RCML-EL-based estimation algorithm given in [7]. We plot the normalized SCNR (ρ), stated in (10), as a function of training data size n, the normalized Doppler, and the normalized angle. For all the plots we are simulating in the regime, where $n = \mathcal{O}(p)$, i.e., $1/10 < p/n < 1$. We also demonstrate the computation times for our proposed algorithm and the RCML-EL algorithm for various n.

In Section IV-B, we compute the target detection probabilities over a range of false alarm probabilities and SCNR. In Section IV-C, we compute the error variance of the minimum variance distortionless response beamformer using the proposed algorithm and compare it with the error variance corresponding to the RCML-EL algorithm and the true covariance matrix.

We compare with the RCML-EL algorithm because it outperforms the sample covariance matrix SMI, FML [59], Chen's algorithm [60], and AIC [50], as documented in [7] in all metrics. In addition, we demonstrate that the proposed algorithm has higher SCNR than the DL method. The DL method adds a small positive perturbation $\zeta \mathbf{I}$ to the sample covariance matrix $\hat{\mathbf{R}}$ to construct the estimator $\bar{\mathbf{R}} = \hat{\mathbf{R}} + \zeta \mathbf{I}$. It has smaller computation time than the proposed algorithm, but yields lower SCNR. The SCNR of the DL method depends on the perturbation ζ, which is scenario-dependent and the optimal ζ lies between the maximum and minimum eigenvalues of the sample covariance matrix, as stated in [61]. We plot two instances where the SCNR is maximum (DL_{max}) and minimum (DL_{min}) by varying the perturbation ζ between the maximum and minimum eigenvalues of the sample covariance matrix.

Since the theory underlying Theorem 1 holds only in the regime of $n > p$, no definitive statements can be made for the case of $n < p$. Therefore, the validity of the proposed algorithm is restricted to the case of $n > p$.

We simulated our results Matlab-R2021b[4] on Windows-11 OS running on AMD Ryzen 7 5800H microprocessor with 16 GB RAM.

[4]All the simulations are completely reproducible. The code is on https://github.com/sjain474/Radar-Clutter-Nonlinear-Shrinkage-Approach.git. For access to the Challenge Dataset contact the coauthor S. Gogineni.

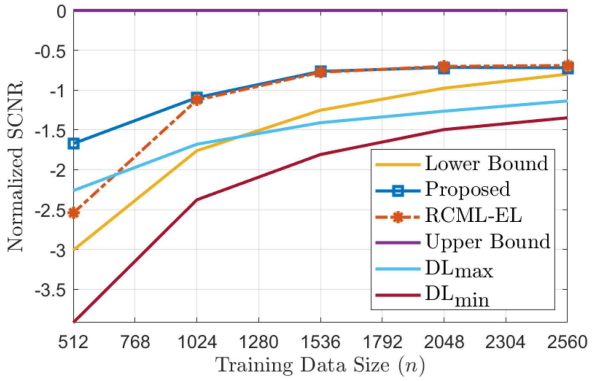

Fig. 4. Proposed algorithm has identical SCNR compared to the RCML-EL algorithm. SCNR for both estimators is within the derived bounds. The SCNR of diagonal loading method is less than proposed algorithm.

A. SCNR Performance

The challenge dataset contains radar target and clutter returns generated by RFView. The scenario in challenge dataset has four targets and ground clutter containing buildings. This scenario involves an airborne monostatic radar flying over the Pacific Ocean near the coast of San Diego looking down for ground moving targets. The data spans several coherent processing intervals as the platform is moving with constant velocity along the coastline. In Tables II–IX, Appendix we state all the parameters used for this scenario.

The challenge dataset consists of a $32 \times 64 \times 2335$ data cube which has the clutter impulse response over 32 channels with 64 pulses and 2335 data samples. We concatenate 8 channels to get a clutter impulse response matrix of size 512×2335. We convolve the rows of the clutter impulse response matrix with a waveform of pulse length 1000 to get a clutter return signal of dimension 512×3334. To the clutter return signal from the challenge dataset we add additive white Gaussian noise with zero-mean and variance $\sigma^2 = 5 \times 10^{-14}$, to get the clutter plus noise return signal. The additive white Gaussian noise is the thermal noise encountered during the measurement of the radar return signal. The thermal noise is chosen using the 6-dB criteria, as stated in [14] and [15] and cannot be zero. The dimension of the clutter plus noise covariance matrix is 512×512. We vary n in the multiples of p till $n < 3334$ to get the sample covariance matrix. For each plot, we use 1024 Monte Carlo simulations. For normalized Doppler, we fix the angle interval at $\frac{\pi}{180}$ and marginalize over it. For the normalized angle, we fix the Doppler interval at $\frac{\pi}{50}$ and marginalize over it. For both cases, we fix $n = 1024$.

Fig. 4 displays the average normalized SCNR versus the number of data samples n. The run-time for different n is given in Table I. Normalized SCNR versus normalized Doppler is given in Fig. 5 and normalized SCNR versus normalized angle in Fig. 6.

The proposed algorithm has higher SCNR performance than the DL method because it has similar SCNR performance to the RCML-EL algorithm, which outperforms the

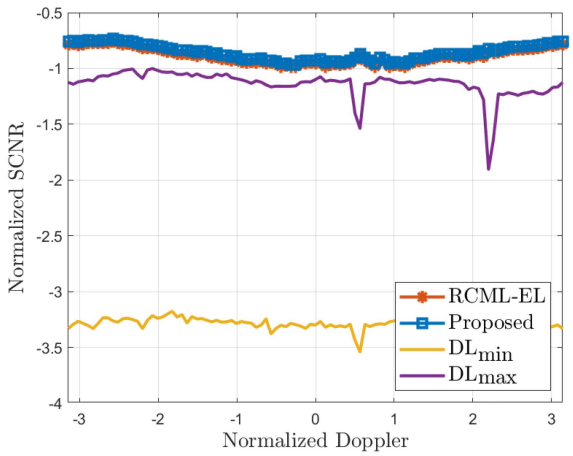

Fig. 5. Algorithm 1 has identical SCNR compared to the RCML-EL algorithm. The SCNR of diagonal loading method is less than proposed algorithm.

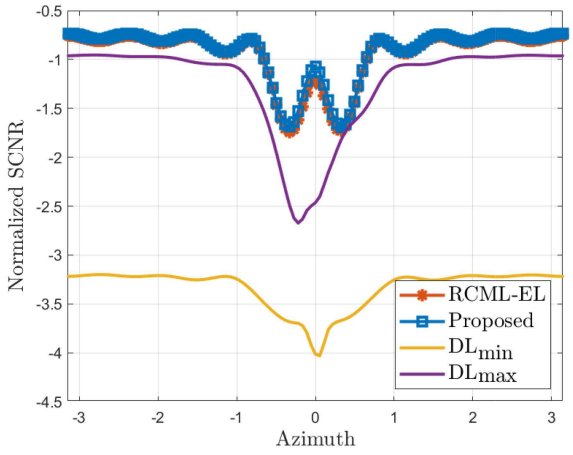

Fig. 6. Algorithm 1 has identical SCNR compared to the RCML-EL algorithm. The SCNR of Diagonal Loading method is less than proposed algorithm.

EigenCanceller [6], [23]. The EigenCanceller and the DL method are similar according to [61].

B. Target Detection

In this section, we use results from Section III-D with the target having a Doppler of $f_d = 0.2$ and an angle of $\theta = 30^\circ$. We plot the target detection probability P_D as we vary false alarm probability P_{FA} from 10^{-5} to 10^{-1} in the multiples of 10 from SCNR $= -10$ dB to 30 dB. We use $n = 1024$ data samples with 1024 Monte Carlo Simulations.

The challenge dataset contains four targets. We consider detecting a single target with remaining targets constituting contaminating clutter discretes. These contaminating clutter discretes do not share the same characteristics as the target of interest so there is no self-target cancellation. Recall from Section III-D that the contaminating clutter discretes change the clutter rank to an unknown $\hat{r}$. By introducing multiple targets as contaminating clutter discretes we demonstrate the robustness of the detector.

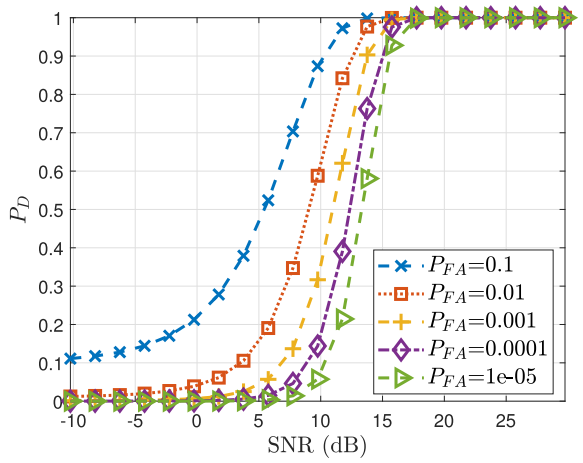

Fig. 7. As P_{FA} is decreased, higher SNR is required to get a fixed P_D for a single target. The presence of other targets is not affecting the detection probabilities as they are projected into the null space of the target subspace. This empirically shows that the detector is robust to the presence of contaminating clutter discretes.

The detection probabilities are the same for both the RCML-EL algorithm, the proposed algorithm and the DL method as the detector uses only the eigenvectors of the sample covariance matrix. The detection probabilities are illustrated in Fig. 7.

C. Empirical Error Variance

In this section, we empirically present the MVDR error variance due to the proposed algorithm with the error variance of the beamformer of the RCML-EL algorithm and the true covariance matrix. The error variance for the beamformer is

$$\text{Error Variance} = 1/|\mathbf{s}^H \mathbf{M}^{-1}\mathbf{s}| \tag{33}$$

where $\mathbf{M} = \bar{\mathbf{R}}_{\text{proposed}}$ for the proposed algorithm, $\bar{\mathbf{R}}_{\text{RCML-EL}}$ for the RCML-EL algorithm and $\mathbf{R}$ for the true covariance matrix, respectively. The target signal $\mathbf{s}$, as defined like $\mathbf{y}_t$ in (10), has Doppler $f_d = 0.3$ and angle $\theta = 30^\circ$. In Fig. 8, the error variance for RCML-EL and the proposed algorithm is identical to the true covariance matrix. The error variance does not change as the training data size is increased since we are working in the asymptotic regime. This is due to the fact that in the asymptotic regime, the estimated covariance matrix converges to the true covariance matrix with probability 1. Hence, the error variance in (33) merely becomes the reciprocal of the SNR from (10) when $\bar{\mathbf{R}} = \mathbf{R}$. Observe that the error variance of DL is higher than the proposed and the RCML-EL algorithm.

To conclude this section, we demonstrated that with reduced covariance computation time, Algorithm 1 gives identical SCNR performance compared to the EL-based covariance estimation algorithm within the proposed bounds. However, the noise computation step requires some precomputed values of the medians of Marchenko Pastur distributions for various values of γ. This also makes our algorithm less robust to a sudden change in the parameters of the

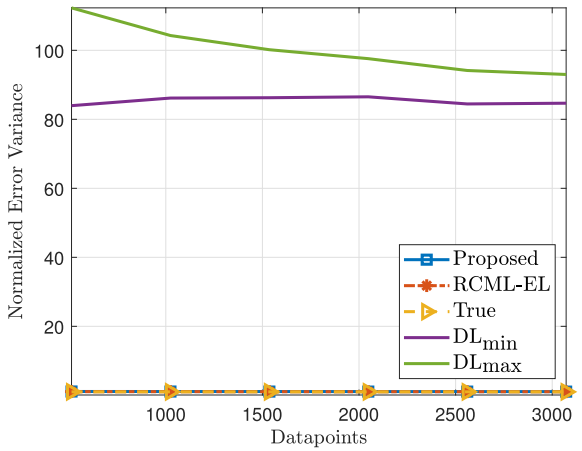

Fig. 8. Normalized error variance due to the proposed algorithm and the RCML-EL algorithm is identical to that of the true covariance matrix. We normalize error variance in (33) by the error variance of the true covariance matrix. The mse of diagonal loading is higher than both RCML-EL and the proposed algorithm.

scenario as data samples can vary depending on the range swath.

We demonstrated the target detection probabilities for different false alarm probabilities using the LR-ANMF detector. We empirically demonstrated the robustness with respect to contaminating clutter discretes in the challenge dataset. We empirically demonstrated that the error variance of the proposed algorithm is identical to the true covariance matrix.

V. CONCLUSION

In this article, we exploit the spiked covariance structure for the clutter plus noise covariance matrix in a high-dimensional setting and propose a nonlinear shrinkage-based rotation invariant estimator. We state the convergence of the spiked eigenvalues of the estimator. We demonstrated the reduced covariance computation times compared to the RCML-EL algorithm. The proposed algorithm and the RCML-EL algorithm have identical SCNR performance. We employed the LR-ANMF detector for robust target detection and empirically showed that the error variance of the algorithm is identical to the true covariance matrix.

Our proposed algorithm computes covariance matrix using batchwise data. In future work it is worthwhile developing an adaptive version of the algorithm. We will also investigate other kinds of loss functions for various scenarios by introducing various constraints and deriving the concentration bounds for the proposed algorithm. The number of contaminating clutter discretes and their relative strength in the challenge dataset is not sufficient to provide a comprehensive analysis of the robustness feature of the LR-ANMF detector. This facet of the technique will be explored in more detail in the future.

APPENDIX
CHALLENGE DATASET PARAMETERS

In this section, we state the parameters we used for the challenge dataset in Tables II–IX. The scenario of the challenge dataset is illustrated in Fig. 9.

TABLE II
Radar Platform Location

Latitude	32.66 deg. N
Longitude	118 deg. W
Height	6000 m
Speed	100 m/s
Azimuth angle of velocity vector (deg. w.r.t. true north)	0 deg
Elevation angle of velocity vector (deg. w.r.t. horizon)	0 deg

TABLE III
Monostatic Radar Parameters for the Challenge Dataset Scenario

Number of Array Elements (Horizontal Dimension)	32
Number of Array Elements (Vertical Dimension)	5
Number of Horizontal Spatial Channels (Receiver)	32
Number of Vertical Spatial Channels (Receiver)	1
Total Number of Spatial Channels (Receiver)	32
Total Number of Channels (Transmitter)	1
Transmit Antenna Gain	503.3509
Receive Antenna Gain	15.7297
Center Frequency	10 GHz
Array Inter-Element Spacing	0.015 m
Number of Coherent Processing Intervals (CPI)	30
Number of Pulses per CPI	64
Pulse Repetition Frequency	1 KHz
Radar Waveform	Standard LFM
Radar Waveform Bandwidth	10 MHz
Radar Waveform Duty Factor	0.1
Sampling Frequency	10000000
Peak Transmit Signal Power	1000 Watts
Number of Range Bins	2334
Size of Data Cubes (for each CPI)	32×64×2334
Range Swath Width	20000 m
Radar Azimuth Look Angle (Fixed)	80.8321 deg
Radar Elevation Look Angle (Fixed)	-5.1364 deg
Clutter Scene Size	20×20 Km
Clutter Patch Size	20×20 m

TABLE IV
First Target is Moving Straight North on the Ground on Ocean Front Walk Near Mission Beach Park in San Diego

Latitude	32.7627 deg. N
Longitude	117.2524 deg. W
Height	0 m
Speed	10 m/s
Azimuth angle of velocity vector (deg. w.r.t. true north)	0
Elevation angle of velocity vector (deg. w.r.t. horizon)	0
RCS	40

TABLE V
Second Target is Moving Straight North on the Ground on Ingraham Street Near Sea World San Diego

Latitude	32.7668 deg. N
Longitude	117.2334 deg. W
Height	0 m
Speed	20 m/s
Azimuth angle of velocity vector (deg. w.r.t. true north)	0
Elevation angle of velocity vector (deg. w.r.t. horizon)	0
RCS	40

TABLE VI
Third Target is Moving South in the Water Off the Coast of San Diego

Latitude	32.793 deg. N
Longitude	117.283 deg. W
Height	0 m
Speed	10 m/s
Azimuth angle of velocity vector (deg. w.r.t. true north)	180
Elevation angle of velocity vector (deg. w.r.t. horizon)	0
RCS	20

It is a weaker target compared to the other targets in this simulation.

TABLE VII
Fourth Target is Moving North in the Water Off the Coast of San Diego

Latitude	32.763 deg. N
Longitude	117.283 deg. W
Height	0 m
Speed	15 m/s
Azimuth angle of velocity vector (deg. w.r.t. true north)	0
Elevation angle of velocity vector (deg. w.r.t. horizon)	0
RCS	30

TABLE VIII
First Clutter Object is an L-Shaped Building Inside Sea World San Diego

Latitude	32.7665 deg. N
Longitude	117.2305 deg. W
Height	6 m
Speed	0 m/s
RCS	50

TABLE IX
Second Clutter Object is a Cube Shaped Building Off Mission Blvd in San Diego

Latitude	32.7901 deg. N
Longitude	117.252 deg. W
Height	6 m
Speed	0 m/s
RCS	50

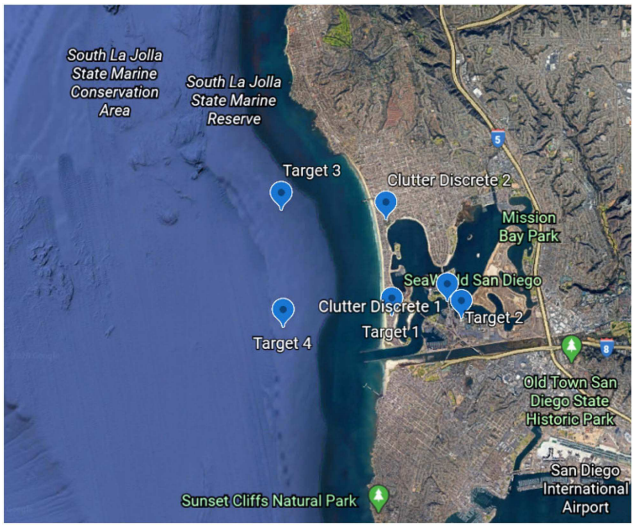

Fig. 9. Challenge dataset scenario consists of four targets and two clutter discretes.

ACKNOWLEDGMENT

The authors would like to thank Dr. Erik Blasch for useful technical discussions.

REFERENCES

[1] I. M. Johnstone, "On the distribution of the largest eigenvalue in principal components analysis," *Ann. Statist.*, vol. 29, no. 2, pp. 295–327, 2001.
[2] D. Paul, "Asymptotics of sample eigenstructure for a large dimensional spiked covariance model," *Statistica Sinica*, pp. 1617–1642, 2007.
[3] D. Donoho, M. Gavish, and I. Johnstone, "Optimal shrinkage of eigenvalues in the spiked covariance model," *Ann. Statist.*, vol. 46, no. 4, pp. 1742–1778, 2018, doi: 10.1214/17-AOS1601.
[4] (Accessed: 2022-12-02.) [Online], Available: https://rfview.islinc.com/RFView/login.jsp
[5] S. Gogineni et al., "High fidelity RF clutter modeling and simulation," *IEEE Aerosp. Electron. Syst. Mag.*, vol. 37, pp. 24–43, Nov. 2022.
[6] B. Kang, V. Monga, and M. Rangaswamy, "Rank-constrained maximum likelihood estimation of structured covariance matrices," *IEEE Trans. Aerosp. Electron. Syst.*, vol. 50, no. 1, pp. 501–515, Jan. 2014.
[7] B. Kang, V. Monga, M. Rangaswamy, and Y. Abramovich, "Expected likelihood approach for determining constraints in covariance estimation," *IEEE Trans. Aerosp. Electron. Syst.*, vol. 52, no. 5, pp. 2139–2156, Oct. 2016.
[8] S. Haykin, *Cognitive Dynamic Systems: Perception-Action Cycle, Radar and Radio*. Cambridge, U.K.: Cambridge Univ. Press, 2012.
[9] V. Krishnamurthy, K. Pattanayak, S. Gogineni, B. Kang, and M. Rangaswamy, "Adversarial radar inference: Inverse tracking, identifying cognition, and designing smart interference," *IEEE Trans. Aerosp. Electron. Syst.*, vol. 57, no. 4, pp. 2067–2081, Aug. 2021.
[10] J. Wintenby and V. Krishnamurthy, "Hierarchical resource management in adaptive airborne surveillance radars," *IEEE Trans. Aerosp. Electron. Syst.*, vol. 42, no. 2, pp. 401–420, Apr. 2006.
[11] I. Reed, J. Mallett, and L. Brennan, "Rapid convergence rate in adaptive arrays," *IEEE Trans. Aerosp. Electron. Syst.*, vol. AES- 10, no. 6, pp. 853–863, Nov. 1974.
[12] Y. I. Abramovich and A. Nevrev, "An analysis of effectiveness of adaptive maximization of the signal-to-noise ratio which utilizes the inversion of the estimated correlation matrix," *Radio Eng. Electron. Phys.*, vol. 26, no. 12, pp. 67–74, 1981.

[13] B. A. Johnson and Y. I. Abramovich, "A matrix extension built under-sampled likelihood ratio test with application to music breakdown prediction and cure," *J. Commun.*, vol. 2, no. 3, pp. 64–72, 2007.
[14] Y. I. Abramovich, "A controlled method for adaptive optimization of filters using the criterion of maximum signal-to-noise ratio," *Radio Eng. Elect. Phys.*, vol. 26, no. 3, pp. 87–95, 1981.
[15] B. D. Carlson, "Covariance matrix estimation errors and diagonal loading in adaptive arrays," *IEEE Trans. Aerosp. Electron. Syst.*, vol. 24, no. 4, pp. 397–401, Jul. 1988.
[16] M. C. Wicks, M. Rangaswamy, R. Adve, and T. B. Hale, "Space-time adaptive processing: A knowledge-based perspective for airborne radar," *IEEE Signal Process. Mag.*, vol. 23, no. 1, pp. 51–65, Jan. 2006.
[17] F. Gini and M. Rangaswamy, *Knowledge Based Radar Detection, Tracking and Classification*. Hoboken, NJ, USA: Wiley, 2008.
[18] J. Ward, "Space-time adaptive processing for airborne radar," in *Proc. Int. Conf. Acoust., Speech, Signal Process.*, vol. 5, pp. 2809–2812, 1994, doi: 10.1109/ICASSP.1995.479429.
[19] R. C. DiPietro, "Extended factored space-time processing for airborne radar systems," in *Conf. Rec. 26th Asilomar Conf. Signals, Syst. Comput.*, 1992, pp. 425–426.
[20] I. P. Kirsteins and D. W. Tufts, "Adaptive detection using low rank approximation to a data matrix," *IEEE Trans. Aerosp. Electron. Syst.*, vol. 30, no. 1, pp. 55–67, Jan. 1994.
[21] J. S. Goldstein, I. S. Reed, and L. L. Scharf, "A multistage representation of the Wiener filter based on orthogonal projections," *IEEE Trans. Inf. Theory*, vol. 44, no. 7, pp. 2943–2959, Nov. 1998.
[22] J. R. Roman, M. Rangaswamy, D. W. Davis, Q. Zhang, B. Himed, and J. H. Michels, "Parametric adaptive matched filter for airborne radar applications," *IEEE Trans. Aerosp. Electron. Syst.*, vol. 36, no. 2, pp. 677–692, Apr. 2000.
[23] A. Haimovich, "The eigencanceler: Adaptive radar by eigenanalysis methods," *IEEE Trans. Aerosp. Electron. Syst.*, vol. 32, no. 2, pp. 532–542, Apr. 1996.
[24] H. Wang and L. Cai, "On adaptive spatial-temporal processing for airborne surveillance radar systems," *IEEE Trans. Aerosp. Electron. Syst.*, vol. 30, no. 3, pp. 660–670, Jul. 1994.
[25] M. J. Wainwright, *High-Dimensional Statistics: A. Non-Asymptotic Viewpoint*. Cambridge, U.K.: Cambridge Univ. Press, 2019, vol. 48.
[26] R. Vershynin, *High-Dimensional Probability: An Introduction With Applications in Data Science*. Cambridge, U.K.: Cambridge Univ. Press, 2018, vol. 47.
[27] Z. Bai and J. W. Silverstein, *Spectral Analysis of Large Dimensional Random Matrices*. Berlin, Germany: Springer, 2010, vol. 20.
[28] W. Wang and J. Fan, "Asymptotics of empirical eigenstructure for high dimensional spiked covariance," *Ann. Statist.*, vol. 45, no. 3, 2017, Art. no. 1342.
[29] A. Tulino and S. Verdú, "Random matrix theory and wireless communications," 2004.
[30] R. Couillet, F. Pascal, and J. W. Silverstein, "A joint robust estimation and random matrix framework with application to array processing," in *Proc. IEEE Int. Conf. Acoust., Speech Signal Process.*, 2013, pp. 6561–6565.
[31] O. Ledoit and M. Wolf, "Optimal estimation of a large-dimensional covariance matrix under Stein's loss," *Bernoulli*, vol. 24, no. 4B, pp. 3791–3832, 2018.
[32] O. Ledoit and M. Wolf, "Quadratic shrinkage for large covariance matrices," *Bernoulli*, vol. 28, no. 3, pp. 1519–1547, 2022.
[33] O. Ledoit and M. Wolf, "Nonlinear shrinkage of the covariance matrix for portfolio selection: Markowitz meets Goldilocks," *Rev. Financial Stud.*, vol. 30, no. 12, pp. 4349–4388, 2017.
[34] O. Ledoit and M. Wolf, "The power of (non-) linear shrinking: A review and guide to covariance matrix estimation," *J. Financial Econometrics*, vol. 20, no. 1, pp. 187–218, 2022.
[35] O. Ledoit and M. Wolf, "A well-conditioned estimator for large-dimensional covariance matrices," *J. Multivariate Anal.*, vol. 88, no. 2, pp. 365–411, 2004.
[36] J. Bun, R. Allez, J.-P. Bouchaud, and M. Potters, "Rotational invariant estimator for general noisy matrices," *IEEE Trans. Inf. Theory*, vol. 62, no. 12, pp. 7475–7490, Dec. 2016.
[37] X. Yuan, W. Yu, Z. Yin, and G. Wang, "Improved large dynamic covariance matrix estimation with graphical lasso and its application in portfolio selection," *IEEE Access*, vol. 8, pp. 189179–189188, 2020.
[38] R. Couillet, F. Pascal, and J. W. Silverstein, "Robust estimates of covariance matrices in the large dimensional regime," *IEEE Trans. Inf. Theory*, vol. 60, no. 11, pp. 7269–7278, Nov. 2014.
[39] S. Sen, "Low-rank matrix decomposition and spatio-temporal sparse recovery for STAP radar," *IEEE J. Sel. Topics Signal Process.*, vol. 9, no. 8, pp. 1510–1523, Dec. 2015.
[40] K. Duan, H. Yuan, H. Xu, W. Liu, and Y. Wang, "Sparsity-based non-stationary clutter suppression technique for airborne radar," *IEEE Access*, vol. 6, pp. 56162–56169, 2018.
[41] B. Kang, V. Monga, and M. Rangaswamy, "Constrained ML estimation of structured covariance matrices with applications in radar stap," in *Proc. IEEE 5th Int. Workshop Comput. Adv. Multi-Sensor Adaptive Process.*, 2013, pp. 101–104.
[42] R. Abrahamsson, Y. Selen, and P. Stoica, "Enhanced covariance matrix estimators in adaptive beamforming," in *Proc. IEEE Int. Conf. Acoust., Speech Signal Process.*, 2007, pp. II–969.
[43] J. R. Guerci, "Cognitive radar: A knowledge-aided fully adaptive approach," in *Proc. IEEE Radar Conf.*, 2010, pp. 1365–1370.
[44] B. Kang, S. Gogineni, M. Rangaswamy, J. R. Guerci, and E. Blasch, "Adaptive channel estimation for cognitive fully adaptive radar," *IET Radar, Sonar Navigation*, vol. 16, no. 4, pp. 720–734, 2022.
[45] J. Guerci, J. Bergin, R. Guerci, M. Khanin, and M. Rangaswamy, "A new MIMO clutter model for cognitive radar," in *Proc. IEEE Radar Conf.*, 2016, pp. 1–6.
[46] B. Nadler, "Finite sample approximation results for principal component analysis: A matrix perturbation approach," *Ann. Statist.*, vol. 36, no. 6, pp. 2791–2817, 2008.
[47] F. Benaych-Georges and R. R. Nadakuditi, "The eigenvalues and eigenvectors of finite, low rank perturbations of large random matrices," *Adv. Math.*, vol. 227, no. 1, pp. 494–521, 2011.
[48] L. Yang, M. R. McKay, and R. Couillet, "High-dimensional MVDR beamforming: Optimized solutions based on spiked random matrix models," *IEEE Trans. Signal Process.*, vol. 66, no. 7, pp. 1933–1947, Apr. 2018.
[49] B. D. Robinson, R. Malinas, and A. O. Hero, "Space-time adaptive detection at low sample support," *IEEE Trans. Signal Process.*, vol. 69, pp. 2939–2954, 2021.
[50] H. Akaike, "A new look at the statistical model identification," *IEEE Trans. Autom. Control*, vol. 19, no. 6, pp. 716–723, Dec. 1974.
[51] P. D. Grünwald, *The Minimum Description Length Principle*. Cambridge, MA, USA: MIT press, 2007.
[52] M. Wax and T. Kailath, "Detection of signals by information theoretic criteria," *IEEE Trans. Acoustics, Speech, Signal Process.*, vol. 33, no. 2, pp. 387–392, Apr. 1985.
[53] Z.-D. Bai, P. R. Krishnaiah, and L.-C. Zhao, "On rates of convergence of efficient detection criteria in signal processing with white noise," *IEEE Trans. Inf. Theory*, vol. 35, no. 2, pp. 380–388, Mar. 1989.
[54] A. A. Shah and D. W. Tufts, "Determination of the dimension of a signal subspace from short data records," *IEEE Trans. Signal Process.*, vol. 42, no. 9, pp. 2531–2535, Sep. 1994.
[55] S. Kay, "Exponentially embedded families-new approaches to model order estimation," *IEEE Trans. Aerosp. Electron. Syst.*, vol. 41, no. 1, pp. 333–345, Jan. 2005.
[56] D. L. Donoho and B. Ghorbani, "Optimal covariance estimation for condition number loss in the spiked model," 2018, *arXiv:1810.07403*.
[57] P. Vallet, G. Ginolhac, F. Pascal, and P. Forster, "An improved low rank detector in the high dimensional regime," in *Proc. IEEE Int. Conf. Acoust., Speech Signal Process.*, 2019, pp. 5336–5340.
[58] M. Rangaswamy, F. C. Lin, and K. R. Gerlach, "Robust adaptive signal processing methods for heterogeneous radar clutter scenarios," *Signal Process.*, vol. 84, no. 9, pp. 1653–1665, 2004.

[59] M. Steiner and K. Gerlach, "Fast converging adaptive processor or a structured covariance matrix," *IEEE Trans. Aerosp. Electron. Syst.*, vol. 36, no. 4, pp. 1115–1126, Oct. 2000.
[60] P. Chen, M. C. Wicks, and R. Adve, "Development of a statistical procedure for detecting the number of signals in a radar measurement," *IEE Proceedings: Radar, Sonar Navigation*, vol. 148, no. 4, pp. 219–226, 2001.
[61] J. Li and P. Stoica, *Robust Adaptive Beamforming*. Hoboken, NJ, USA: Wiley, 2005.

Shashwat Jain (Student Member, IEEE) received the joint B.Tech and M.Tech degree in electronics and communications engineering from the Indian Institute of Technology, Kharagpur, West Bengal, India, in 2021. He is currently working toward the graduate degree in electrical and computer engineering with the Department of Electrical and Computer Engineering, Cornell University, Ithaca, NY, USA.

His research interests include high-dimensional random matrix theory in signal processing, control of large language models and inverse games.

Mr. Jain was the recipient of the Jacob's Fellowship by Cornell University, Ithaca, NY, USA, and has been a speaker at the 2023 International Conference of Acoustics, Speech, and Signal Processing.

Vikram Krishnamurthy (Fellow, IEEE) received the Ph.D. degree in mathematical systems theory from the Australian National University, Canberra, ACT, Australia, in 1992.

From 2002 to 2016, he was a Professor and Canada Research Chair with the University of British Columbia, Vancouver, BC, Canada. He is currently a Professor with the School of Electrical & Computer Engineering, Cornell University, Ithaca, NY, USA. He is author of the book *Partially Observed Markov Decision Processes* (Cambridge University Press, 2016). His research interests include statistical signal processing and stochastic control in social networks and adaptive sensing.

Dr. Krishnamurthy was the recipient of an Honorary Doctorate from KTH (Royal Institute of Technology), Sweden, in 2013. He served as Distinguished Lecturer for IEEE Signal Processing Society and Editor-in-Chief for IEEE JOURNAL ON SELECTED TOPICS IN SIGNAL PROCESSING.

Muralidhar Rangaswamy (Fellow, IEEE) received the B.E. degree in electronics engineering from Bangalore University, Bangalore, Karnataka, India, in 1985, and the M.S. and Ph.D. degrees in electrical engineering from Syracuse University, Syracuse, NY, USA, in 1992.

He has held various industrial and academic appointments. He is currently the Technical Lead for Radar Sensing with the RF Technology Branch within the Sensors Directorate of the Air Force Research Laboratory, Wright Patterson Air Force Base, Dayton, OH, USA. He developed innovative techniques to address the challenges of his research interests by using physics-based approaches and exploiting underlying structure in the data gained from a priori information. He has coauthored more than 300 refereed journal and conference record papers in the areas of his research interests. In addition, he has authored or coauthored nine books and has coinvented three U.S. patents. His research interests include radar signal processing, spectrum estimation, modeling non-Gaussian interference phenomena, and statistical communication theory. A common theme of his research in these areas is that of Big Data. A large class of radar signal processing problems incurs the curse of dimensionality, namely, the training data requirement and computational cost grow explosively with increasing dimensionality.

Dr. Rangaswamy was the recipient of the NATO Scientific Excellence award in 2022, IEEE-AESS Harry Rowe Mimno award in 2021, the NATO SET Technical Panel Team Excellence award in 2021, the 2020 IEEE Dayton Section Fritz Russ memorial award, the 2019 Technical Cooperation Panel award from the Office of Secretary of Defense, the 2019 International Society for Information Fusion Jean-Pierre Le Cadre Best Paper award, 2013 IEEE Warren White Radar Award, the 2013 Affiliate Societies Council Dayton Outstanding Scientist and Engineer Award, the 2007 IEEE Region 1 Award, the 2006 IEEE Boston Section Distinguished Member Award, and the 2005 IEEE-AESS Fred Nathanson memorial outstanding young radar engineer award. He was also the recipient of the 2012 and 2005 Charles Ryan basic research award from the Sensors Directorate of AFRL, in addition to more than 40 scientific achievement awards. He has an h-index of 41 and i-10 index of 118. He was the recipient of a service recognition for his role as the Technical Editor for IEEE TRANSACTIONS ON AEROSPACE AND ELECTRONIC SYSTEMS, in 2016. In 2021, he was ranked 887 out of 161 179 (scientists in his field) by a Stanford University survey of scientists worldwide who are in the top 2% of their field. He served as the Technical Editor (Associate Editor-in-Chief) for Radar Systems in IEEE TRANSACTIONS ON AEROSPACE AND ELECTRONIC SYSTEMS (IEEE-TAES), from 2007 to 2015, and as Associate Editor for Radar Systems within IEEE-TAES, from 2004 to 2007. He was the Co-Editor-in-Chief for the *Digital Signal Processing* journal, between 2005 and 2011. He was a member of the Senior Editorial Board of IEEE JOURNAL OF SELECTED TOPICS IN SIGNAL PROCESSING, from 2012 to 2014. He was a two-term elected member of the sensor array and multichannel processing technical committee (SAM-TC) of the IEEE Signal Processing Society, between 2005 and 2010, and served as a member of the Radar Systems Panel (RSP) in the IEEE-AES Society, from 2006 to 2019. He was the General Chairman for the 4th IEEE Workshop on Sensor Array and Multichannel Processing (SAM-2006), Waltham, MA, USA, July 2006. He has served on the Technical Committee of the IEEE Radar Conference series in a myriad of roles (Track Chair, Session Chair, Special Session Organizer and Chair, Paper Selection Committee Member, Tutorial Lecturer). He served as the Publicity Chair for the First IEEE International Conference on Waveform Diversity and Design, Edinburgh, U.K. November 2004. He served on the conference subcommittee of the RSP. He was the Technical Program Chairman for the 2014 IEEE Radar Conference.

Bosung Kang (Member, IEEE) received the B.S. and M.S. degrees in electrical and electronic engineering from Yonsei University, Seoul, South Korea, in 2005 and 2007, respectively, and the Ph.D. degree in electrical engineering from The Pennsylvania State University, University Park, PA, USA, in 2015.

He was with LG Electronics, Seoul, South Korea, as a Research Engineer, from 2007 to 2011. He is currently a support contractor with Air Force Research Laboratory, Wright Patterson Air Force Base, Dayton, OH, USA, and a Senior Radar Engineer with the University of Dayton Research Institute, Dayton, OH, USA. He developed image and video signal processing algorithms in mobile camera and monitor applications. His research interests include statistical signal processing, detection and estimation, convex optimization, and radar signal processing with applications to radar and communication systems.

Dr. Kang was the recipient of the First Place in the Student Paper Competition at the IEEE Radar Conference, Cincinnati, OH, USA, in 2014. He was also the recipient of the 2015 Robert T. Hill Best Dissertation Award presented by IEEE Aerospace and Electronic Systems Society and 2022 IEEE Dayton Section Aerospace and Electronic Systems Award by the IEEE Dayton Section. He has served as a Reviewer for several reputed IEEE journals and conferences.

Sandeep Gogineni (Senior Member, IEEE) received the B.Tech. degree in electronics and communications engineering, International Institute of Information Technology Hyderabad, Hyderabad, Telangana, India, in 2007, the M.S. and Ph.D. degrees in electrical engineering from Washington University in St. Louis, St. Louis, MO, USA, in 2009 and 2012, respectively.

He is a Research Scientist with Information Systems Laboratories, Poway, CA, USA, with over 15 years of experience working on radar and wireless communications systems. He has worked for six years as an on-site contractor for Air Force Research Laboratory, Wright Patterson Air Force Base, Dayton, OH, USA, developing novel signal processing algorithms and performance analysis for passive radar systems. In addition, he and his colleagues at ISL have demonstrated the use of neural networks and artificial intelligence techniques to solve extremely challenging RF sensing problems. His expertise includes statistical signal processing, detection and estimation theory, deep learning, artificial intelligence, performance analysis, and optimization techniques with applications to active and passive RF sensing systems.

Dr. Gogineni was the recipient of IEEE Dayton Section Aerospace and Electronics Systems Society Award for contributions to passive radar signal processing. Prior to his time with AFRL, during his graduate studies at Washington University in St. Louis, he developed optimal waveform design techniques for adaptive MIMO radar systems and demonstrated improved target detection and estimation performance. At ISL, he has been working on high-fidelity RF modeling and simulation, channel estimation algorithms, and optimal probing strategies for MIMO radar systems in the context of cognitive fully adaptive radar.